Computers and Electronics in Agriculture 250 (2026) 111942

Contents lists available at ScienceDirect

Computers and Electronics in Agriculture

journal homepage: www.elsevier.com/locate/compag

Recognition of kiwifruit pruning position based on vine segmentation and dormant bud detection with their planar distribution

Shuolin Kong [a], Bo Jia [a], Qichen Huang [a], Juncai Huang [a], Rui Li [a,1,*], Bao Zhou [b], Xiancun Zhou [b], Zhenchao Wu [c], Jinyong Chen [d], Xiaoxu Sun [d], Dateng Zheng [e], Davut Karayel [f], Dae-Hyun Lee [g], Shen Hin Lim [h], Longsheng Fu [a,b,c,2,*]

[a] College of Mechanical and Electronic Engineering, Northwest A&F University, Yangling, Shaanxi 712100, China
[b] School of Electronic Information and Artificial Intelligence, West Anhui University, Lu'an, Anhui 237012, China
[c] School of Engineering, Anhui Agricultural University, Hefei, Anhui 230036, China
[d] Zhengzhou Fruit Research Institute, Chinese Academy of Agricultural Sciences, Zhengzhou, Henan 450009, China
[e] Jiangxi Provincial Key Laboratory of Modern Agricultural Equipment, Ji'an, Jiangxi 343009, China
[f] Department of Agricultural Machinery and Technologies Engineering, Faculty of Agriculture, Akdeniz University, Antalya 07058, Turkey
[g] Department of Smart Agriculture Systems Machinery Engineering, Chungnam National University, Daejeon 34134, South Korea
[h] School of Engineering, University of Waikato, Hamilton 3240, New Zealand

ARTICLE INFO

Keywords:
Kiwifruit winter pruning
YOLO11x
Vine segmentation
Dormant bud detection
Pruning position recognition

ABSTRACT

Kiwifruit winter pruning is a laborious, seasonal, and irreversible operation. The key to achieving automatic winter pruning of kiwifruit lies in the recognition of pruning position. In this study, a method based on kiwifruit vine segmentation and dormant bud detection with their planar distribution was developed to recognize the pruning position of kiwifruit vine. Firstly, YOLO11x-seg and YOLO11x were applied to segment vines and detect dormant buds, respectively. Secondly, the DBSCAN algorithm was applied to remove wrongly segmented vine, and vine skeleton was then extracted. Thirdly, dormant buds were matched with their corresponding canes based on the overlap ratio, and then ordered from the cane base. Finally, the pruning position was recognized based on the planar distribution of vines and dormant buds. Results showed that YOLO11x-seg and YOLO11x achieved an outstanding performance with segmentation and detection m*AP* of 82.5% and 89.0%, respectively. The method proposed in this study attained pruning position recognition accuracies of 77.3%, 81.8%, and 88.9% under the three pruning strategies of cane short-truncation, lateral cane removal, and cane renewal, respectively. These results indicate that the proposed method is promising for robotic winter pruning of kiwifruit.

1. Introduction

Winter pruning is a labor-intensive and essential operation to maintain orchard health and produce high kiwifruit yields. Kiwifruit pruning is typically categorized into summer and winter pruning, with the latter being particularly critical (Özcan and Uslu, 2010). Winter pruning directly determines production in the coming year, as it involves the redistribution of nutrients and the growth of new vines, which are the basis of fruit production (Patterson and Currie, 2011). However, winter pruning is a laborious, seasonal and irreversible operation that requires many highly qualified and specialized technicians for good pruning. Most research focuses on the impact of pruning on the kiwifruit structure or pruning strategies for different varieties (Patiyal et al., 2024), with a lack of research on recognizing pruning positions.

Vision-based perception systems have been successfully applied in agricultural robots for tasks such as weeding, pollination, and harvesting (Fang et al., 2023; Gao et al., 2025; Ray et al., 2025; Thakur et al., 2023). However, automated kiwifruit pruning requires accurate recognition of pruning positions, which depends on the joint recognition of fine-scale vine structures and small buds within the canopy. To date, research on kiwifruit pruning position recognition remains at an early stage, and the key technical challenges of simultaneously performing vine structure

* Corresponding authors.
E-mail addresses: ruili1216@nwafu.edu.cn (R. Li), fulsh@nwafu.edu.cn (L. Fu).
[1] ORCID: 0000-0003-1329-9817.
[2] ORCID: 0000-0003-3253-2637.

https://doi.org/10.1016/j.compag.2026.111942
Received 10 January 2026; Received in revised form 13 May 2026; Accepted 21 May 2026
Available online 28 May 2026
0168-1699/© 2026 Elsevier B.V. All rights are reserved, including those for text and data mining, AI training, and similar technologies.

segmentation and small bud detection to support pruning decision-making have not been fully explored. Consequently, a vision-based system capable of making strategy-specific pruning decisions for kiwifruit and suitable for real-time robotic operation is still lacking.

The crucial step in automatic pruning position recognition is to obtain the structural information of kiwifruit vines. In the study of vine recognition through point clouds, Medeiros et al. (2017) acquired structural point cloud data of apple trees with an accuracy of 98.0% through laser sensor scanning and a scan time of 30 min. Li et al. (2021) used backpropagation neural network to reconstruct point clouds of apple tree branches with an accuracy of 85.7%. Williams et al. (2023) acquired images from both sides of grapevines to reconstruct grapevine point clouds and the reconstruction still took more than 10 min. While point clouds have been utilized for tree branch reconstruction, their processing speed remains relatively slow.

Segmenting vines in images is more suitable, as previous studies have attempted to use deep learning techniques for vine segmentation in images to obtain two-dimensional structural information. Efforts have been made to segment branches in images using deep learning techniques. Song et al. (2021) adopted DeepLabV3 + to segment calyxes and vines on kiwifruit images, achieving an intersection over union (IoU) of 68.0% and 70.0%, respectively. Borrenpohl and Karkee (2023) utilized Mask R-CNN to segment branches in sweet cherry trees with upright fruiting offshoots architecture, which reached an accuracy of 89.0%. Carneiro et al. (2022) segmented grapevines based on Unet and achieved an IoU of 91.6%. As deep learning continues to advance, YOLO (You Only Look Once) architectures have been widely recognized for their effectiveness in instance segmentation (Shen et al., 2025; Chen et al., 2025;). Therefore, considering the advantages of YOLO series models in terms of ease of deployment and continuous updates, using YOLO to segment kiwifruit vine is feasible.

After segmenting kiwifruit vines, bud detection is also required to recognize pruning positions. As a vine crop, kiwifruit differs from bush crops such as apple (Karkee et al., 2014; Bai et al., 2019) and cherry (Kefalas et al., 2025), whose methods of pruning position recognition rely only on branch information and thus are not directly applicable. Pruning of kiwifruit requires not only vine segmentation but also dormant bud detection, similar to pruning position recognition in the grapevine. Chen et al. (2024) proposed a two-stage recognition strategy for grapes, which separates the vines and background using PSP-net and detects bud points with YOLOv5. In addition, YOLOv5 has been successfully used to identify sugarcane stems through object detection (Maurya et al., 2025). In summary, under the same backbone, YOLO model can achieve both vine detection and segmentation by only modifying the head network, while maintaining strong performance in both tasks. This demonstrates that YOLO models are well suited for feature extraction of vines, making the use of YOLO series appropriate. Considering that YOLO26 is still under continuous development and lacks sufficient stability, while YOLOv8 is relatively outdated, YOLO11 was initially selected as a balanced and reliable solution.

This study introduces a novel method for the automatic recognition of pruning positions based on kiwifruit vine segmentation and dormant bud detection, as well as their planar distribution. YOLO11x-seg was employed to segment vines, while YOLO11x was employed to detect dormant buds in images, and both were integrated with three winter pruning strategies (cane short-truncation, lateral cane removal and cane renewal) to recognize pruning positions on vines.

2. Materials and methods

This study focused on automatically recognizing the pruning positions for kiwifruit winter pruning. The overall schematic workflow is shown in Fig. 1. Briefly, for the three winter pruning strategies of cane short-truncation, lateral cane removal and cane renewal, the specific method for recognizing pruning positions was proposed. Elaborate descriptions of the method were provided in the subsequent sections.

2.1. Winter pruning strategy

Ensuring healthy plant growth to enhance fruit quality and yield, kiwifruit winter pruning involves the specific strategies of cane short truncation (CST), lateral cane removal (LCR), and cane renewal (CR) based on cane condition. These pruning strategies are informed by practical management experience and recommendations from professional kiwifruit cultivation experts. When there are no lateral canes on cane, as shown in Fig. 2a, the CST strategy is usually employed to retains seven dormant buds to ensure vigorous growth. When lateral canes are distributed on the cane, the LCR strategy is applied by cutting them at the junction between the cane and the lateral cane, thereby minimizing ineffective nutrient consumption, as shown in Fig. 2b. When the first lateral cane on the cane is less than approximately 50 cm from the cordon, as shown in Fig. 2c, the CR strategy is utilized. Under this strategy, the first lateral cane within approximately 50 cm of the cordon is selected as the cane for the next year, while the cane from the previous year is cut off. The CR strategy is a critical step in maintaining fruiting ability and extending tree lifespan, preventing outward migration of fruit parts.

2.2. Data preparation

The kiwifruit canopy images were captured during November-December 2023 from a kiwifruit orchard, Yangling, Shaanxi Province, China (34°17′ N, 108°2′ E). Kiwifruit is cultivated with uniformly designed support frames, resulting in canopies at relatively consistent heights. During winter pruning, kiwifruit is in dormancy with withered leaves, no fruit, and a clear canopy structure. To ensure robustness under varying illumination conditions, image acquisition was conducted at different times of the day, including daytime and dusk, and under

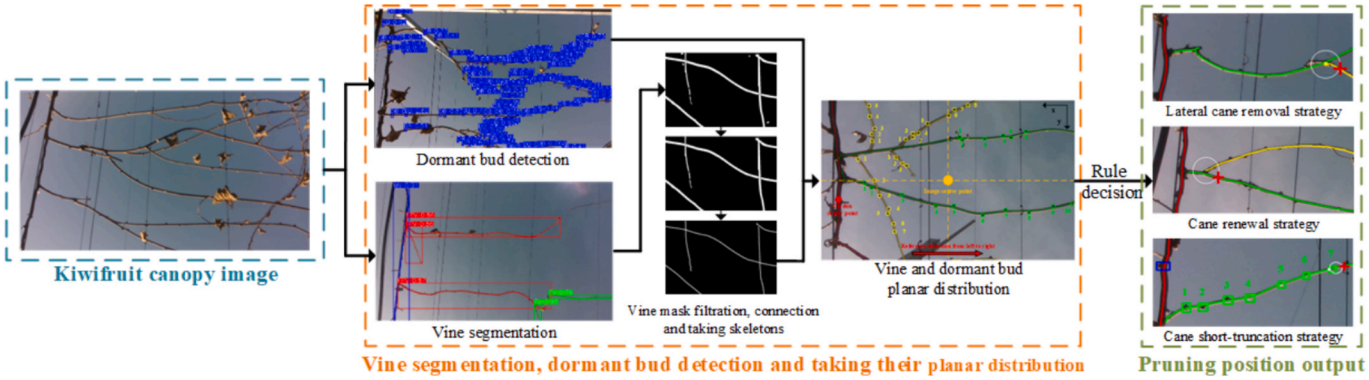


Fig. 1. Kiwifruit winter pruning position recognition pipeline.

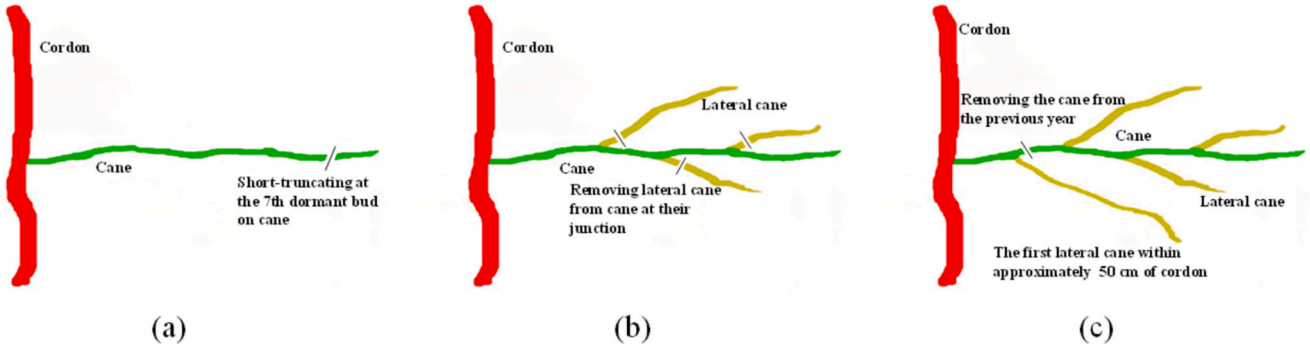


Fig. 2. Kiwifruit winter pruning strategy with (a) the CST strategy, (b) the LCR strategy and (c) the CR strategy.

both sunny and cloudy weather conditions, thereby accounting for the influence of natural lighting variability. In addition, kiwifruit trees with different growth ages ranging from 3 to 5 years were included during image collection to improve dataset diversity and model generalization under varying canopy structures. An RGB-D (Red, Green, Blue, and Depth) camera (RealSense D435, Intel, USA) was held upwards at around 80 cm below the vines and dormant buds. Images were acquired at a sampling density of approximately 3 images per square meter to ensure sufficient canopy coverage. A total of 500 images were collected at different times and saved in 'png' format with a resolution of 1280 × 720 pixels, and all images are available at https://github.com/Smart-Ag/Kiwifruit_pruning_image. Two datasets were developed for this study with the same images but different in annotation and training strategy, one used for was used for kiwifruit vine segmentation (KVS) and the other for dormant bud detection (DBD).

In dataset KVS, 500 images were annotated by using Labelme software (an image labeler toolbox developed by MIT's Computer Science and Artificial Intelligence Laboratory), The annotated categories included the cordon ('CO' – red), cane ('CA' – green), and lateral cane ('LCA' – yellow), which were manually delineated as polygonal regions using vine edges as annotation boundaries, as illustrated in Fig. 3. The cordon is borne on the kiwifruit trunk and is a plant part that bears canes. The cane is attached to the cordon, which is the part from which lateral canes grow. The lateral cane grows from the cane and is the part where kiwifruit is produced. Because the camera inevitably captures the opposite side of the cordon and pruning position recognition is not feasible on this side, only the side with primary pruning positions was annotated. After each image was annotated, the annotation files were saved in 'json' format.

In DBD dataset, dormant buds on canes and lateral canes were manually annotated using Labelme software. Dormant buds are generally conical or oval and slightly protruding, which makes them wider than the surrounding vine. Based on these morphological characteristics, dormant buds ('DB' – blue) were annotated as rectangular boxes, ensuring that each bounding box fully enclosed the entire dormant bud, and the annotation files were saved in 'json' format. Even if a vine was occluded, its polygon extended across the occlusion to encompass the remaining visible part. The DBD dataset contains the same 500 images as those applied in the KVS dataset. An annotated image of dormant buds is shown in Fig. 4.

Overall, a total of 547 cordons, 1431 canes, 1873 lateral canes, and 13,640 dormant buds were annotated in the KSV and DBD datasets, 279 images contained more than eight vines, and 853 vine overlap occurrences were observed, indicating the relatively complex canopy structure and challenging vine occlusion conditions in the dataset. The KSV and DBD datasets were randomly divided into a training set (350 images), validation set (100 images) and testing set (50 images) in a 7:2:1 ratio, with identical images across the training, validation and testing sets in the KSV and DBD datasets to ensure the reliability of evaluation metrics.

Finally, 15 kiwifruit canopy images collected from a separate orchard in Xianyang, Shaanxi Province, in November 2025 were used for cross-orchard validation. These data were excluded from model training and were intended to provide a robustness evaluation of the best performing segmentation and detection models.

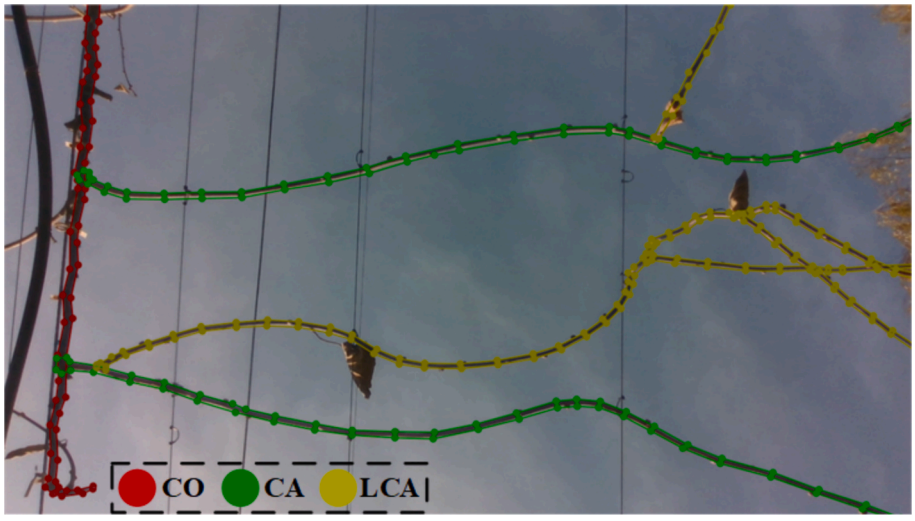


Fig. 3. Kiwifruit vines labeled in a collected canopy image, where the cordon, cane and lateral cane are labeled as 'CO', 'CA', and 'LCA' with red, green, and yellow polygons, respectively.



Fig. 4. Dormant buds labeled in a collected canopy image, where they are labeled as 'DB' with blue rectangular boxes.

2.3. Network training

Two models were trained for vine segmentation and dormant bud detection by employing YOLO11x-large (YOLO11x) and YOLO11x-large instance segmentation network (YOLO11x-seg). YOLO11 and YOLO11x-seg are both convolutional neural network (CNN) structures, where YOLO11x-seg is reached by replacing the detection head with a segmentation head in YOLO11. The training set of KVS was used to train YOLO11x-seg, and the training set of DBD was used to train YOLO11x. These models were initialized with pre-trained weights trained on the COCO (Lin et al., 2014) dataset. The models were trained on a Windows 10 desktop computer with an Intel (R) Xeon (R) Gold 5218 CPU, an Nvidia GeForce RTX 4090 GPU, and 128 GB of RAM. The models were implemented using the PyTorch deep learning framework version 2.0.1. The training parameters of the two models were same, with an input size of 1280*1280 pixels, a batch size of 2, an epoch of 300, a learning rate of 0.001, and a weight decay coefficient of 0.005. The training process employed the Adam optimizer with a linear learning rate decay strategy, ensuring efficient convergence. A non-maximum suppression method was applied to remove overlapping bounding boxes.

2.4. Kiwifruit vine skeleton extraction

The prerequisite for obtaining a complete vine skeleton is to remove incorrectly segmented regions and connect discontinuous vine masks. The resultant dataset has scenarios of uncertain distribution and irregular morphology of incorrectly segmented regions and discontinuity in some vine masks resulting from model performance. As illustrated by vine mask-A in Fig. 5a, the k-means algorithm was deemed unsuitable for such scenarios because it requires a predefined number of clusters (Ruan et al., 2023). Thus, the density-based spatial clustering of applications with noise algorithm (DBSCAN) was employed to remove incorrectly segmented regions with feature similarity among kiwifruit vines. DBSCAN algorithm attained adaptive clustering by analyzing the spatial density distribution of pixel points, without the need to pre-set the number of clusters. The DBSCAN clustered the dense set of points (correctly segmented vines) in an image into one class while classifying the less dense set of points (wrongly segmented vine) into other classes. Subsequently, considering that the gaps between disconnected regions were small, the endpoints of masks on both sides of the gaps were connected to achieve vine reconnection. The reconnected vine mask is shown as vine mask-A in Fig. 5b, while the vine masks for removing wrongly segmented regions are vine mask-B and vine mask-C,

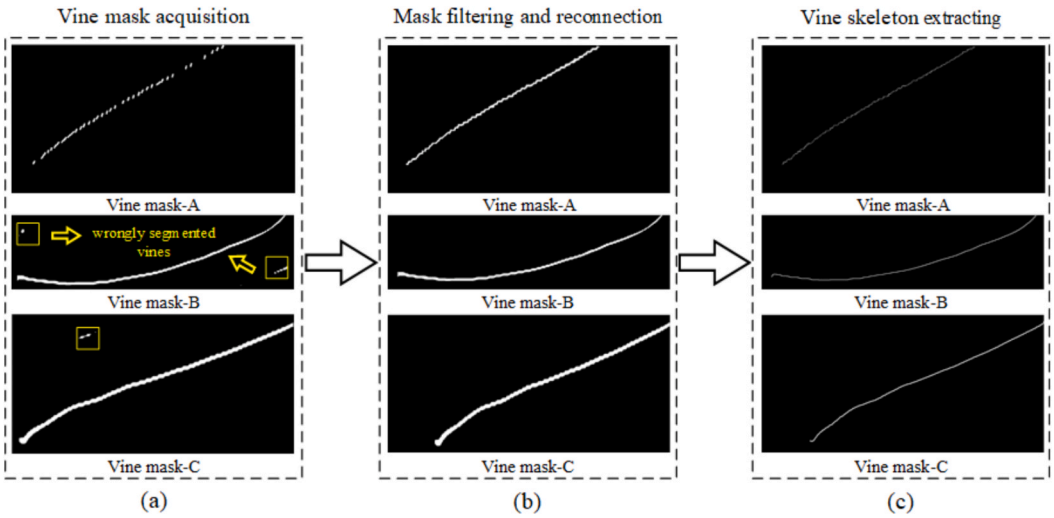


Fig. 5. The process of extracting skeleton of kiwifruit vines, in which (a) vines were segmented with YOLO11x-seg, then (b) filter the erroneous segmented regions through the DBSCAN algorithm and reconnection vine mask, and finally (c) extracting vine skeletons using parallel thinning algorithm.

respectively.

After obtaining a complete vine mask, the vine skeleton was extracted by the thinning skeletonization method from OpenCV. This method could refine a region to a skeleton and generate a refined image representing the centerline of vine. The extracted skeleton, as shown in Fig. 5c, retained the basic morphology of vine.

2.5. Determination of reference direction and dormant bud order

A reference direction of image was determined based on the cordon location in the image to determine the starting position of dormant buds. The growth direction of other vines could be inferred from the position of cordon because the cane is attached to the cordon, and a lateral cane sprouts from a dormant bud on the cane. The reference direction of the image is then determined based on the relative position between the cordon center point and the image center point. After obtaining the reference direction of the image, the endpoints of each vine and the lateral cane growing on the cane are determined based on the reference direction.

A mask-matching method based on the maximum intersection area of dormant buds and canes was proposed to determine their subordination. Due to the random distribution of dormant buds on vines, their bounding boxes overlap with the cane skeleton mask to some extent. By calculating the intersection area between each dormant bud's bounding box and the cane skeletons, dormant buds are attributed to the vine whose skeleton produces the largest intersection area with that dormant bud's bounding box. Bounding boxes of all matched dormant buds belonging to the same cane were ordered according to the reference direction to reflect the actual distribution order of them. The steps for obtaining the reference direction, matching dormant buds and lateral canes, and sorting the dormant buds are detailed in Algorithm 1.

Algorithm 1 (Algorithm of determining reference direction and ordering dormant bud)

Input: Ordinate coordinates of cordon: *Cx*; Ordinate coordinate of image center: *Ix*; Cane skeleton: *Sc*; Lateral cane skeletons: *Sl*; Dormant buds bounding box: *DB*;
Output: Reference direction: *Rd*; Coordinates of cane endpoint: *Ec*; Coordinates of lateral cane endpoint: *El*; Matched lateral cane on cane: *MSl*; Ordered dormant bud: *DBo*;
1. **if** Max(*Cx*) > *Ix* **then**
2. *Rd* ← 'right'
3. **else**
4. *Rd* ← 'left'
5. **end if**
6. get endpoint of *Sc* in the *Rd* as *Ce*;
7. **for** each *DB* and *Sc* **do**
8. compute the intersection area between *DB* and *Sc*;
9. find *DB* that has the maximum intersection area with *Sc*;
10. add *DB* to *DBo*;
11. **end for**
12. sort *DBo* by ordinate coordinate; //in descending order if *Rd* is 'right' or ascending if 'left'
13. **for** each *Sl* **do**
14. get endpoint of *Sl* in the *Rd* as *El*;
15. **end for**
16. **for** each *El* **do**
17. calculate *distance* to closest *Sc*;
18. **if** *distance* ≤ 20 pixels **then**
19. add *Sl* that *El* is closest to *Sc* into *MSl*;
20. **end if**
21. **end for**

Finally, complete vine information is reached by matching lateral canes with the cane within 20 pixels of their endpoints. The value of 20 pixels was obtained by calculating half of the average distance between all detected dormant buds and then rounding down to the nearest integer. The distances used in this study are expressed in pixels rather than real-world units. This choice is motivated by preliminary experiments showing that, in winter, the absence of leaf obstruction exposes the depth camera to direct sunlight, which significantly degrades its performance. Given that kiwifruit vines are tied to wires at fixed heights as the part of orchard management, inferring spatial relationships based on pixel distances is a practical and reliable strategy. The resulting visualization is shown in Fig. 6.

2.6. Pruning position recognition method

After segmenting vines and detecting buds, and following a similar approach to the pruning position recognition study on grapevines conducted by Gentilhomme et al. (2023) and Williams et al. (2023), the pruning strategies defined by experts are transformed into an executable algorithm. Subsequently, a specific pruning position recognition method is inferred according to the relative spatial relationships between canes and lateral canes.

2.6.1. Recognition method under the CST strategy

When there are no lateral canes on cane, it must be retained to develop lateral canes for the following season. Therefore, after ordering dormant buds, the number of dormant buds and cane skeleton mask were combined to recognize pruning position. When a cane does not have any lateral cane, the pruning position is recognized under the CST strategy. This step is detailed in Algorithm 2 and Fig. 7. The offset circle was set to 10 pixels, which is approximately the typical thickness of a cane in the image according to statistics. In future work, if more accurate depth information can be obtained, the actual physical thickness of the cane can be used instead to determine the offset distance more precisely.

Algorithm 2 (Algorithm of recognizing pruning position under the CST strategy)

Input: Reference direction: *Rd*; Cane skeleton: *Sc*; Ordered dormant bud on cane: *DBo*; Matched lateral cane on cane: *MSl*;
Output: Coordinate of pruning position under the CST strategy: *Pcst*;
1: **for** each *Sc* **do**
2: **if** (*MSl* of current *Sc* == Null) **then** // CST strategy
3: *DB7* ← the Coordinates of 7th dormant bud in *DBo*
4: draw an offset circle with a radius of 10 pixels around *DB7*;
5: find the intersection points between the offset circle and *CSc*;
6: **if** (*Rd* == 'right')**then**
7: *Pcst* ← leftmost point in intersection points
8: **else**
9: *Pcst* ← rightmost point in intersection points
10: **end if**
11: **end if**
12: **end for**

2.6.2. Recognition method under the LCR strategy

When the distance between the first lateral cane and the cane endpoint exceeds 250 pixels, lateral canes beyond this threshold are pruned to prevent the outward displacement of the fruiting zone in the following season. Under this condition, the LCR strategy is triggered, and the pruning position on the lateral cane is subsequently recognized. This step is detailed in Algorithm 3 and Fig. 8. The 50 cm distance between the cane and its lateral cane endpoints specified by the LCR strategy represents the distance from the first to the seventh bud. According to statistics from bud detection in this study, this distance corresponds to approximately 200 pixels in the images. Given that manual pruning often leaves extra buds on the cane, a threshold of 250 pixels is appropriate for pruning strategy decisions. In addition, the offset circle radius is set to 30 pixels to ensure a sufficient safety margin during pruning and to prevent accidental cutting of the lateral cane intended for retention. The value of 30 pixels was obtained by calculating half of the average distance between all detected dormant buds and then rounding up to the nearest integer.

Algorithm 3 (Algorithm of recognizing pruning position under the LCR strategy)

Input: Coordinates of lateral cane skeletons: *Sl*; Coordinates of current cane endpoint: *Ec*; Coordinates lateral cane endpoint: *El*;
Output: Coordinate of pruning position under the LCR strategy: *Plcr*;
1: **for** each *El* **do**
2: Compute distance *d* between *El* and *Ec*

(*continued on next page*)

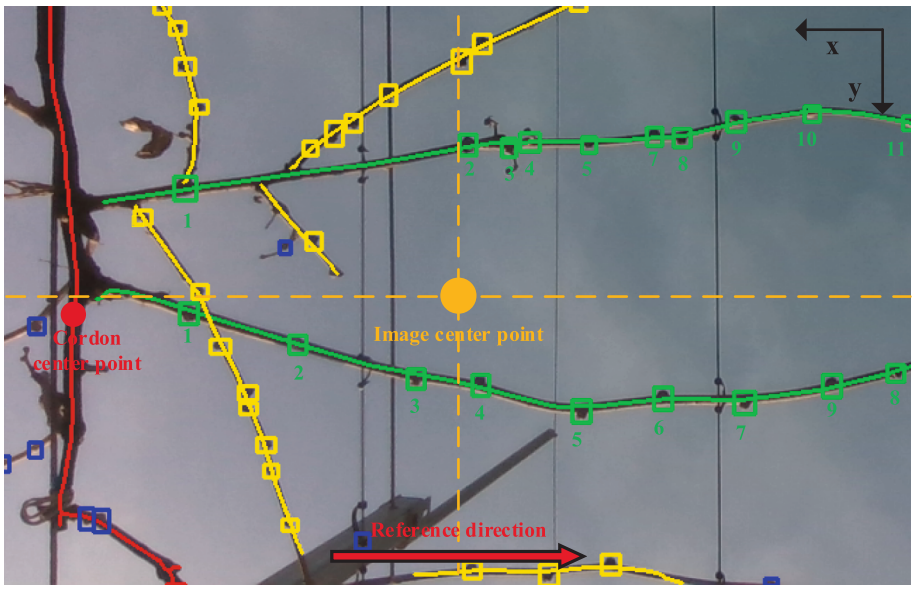


Fig. 6. Visualization of reference direction and ordered dormant buds, where the green, red and yellow line represent skeleton of cane, cordon and lateral cane, respectively. Green, yellow and bule boxes represent dormant buds in cane, lateral cane, and unmatched dormant buds, respectively.

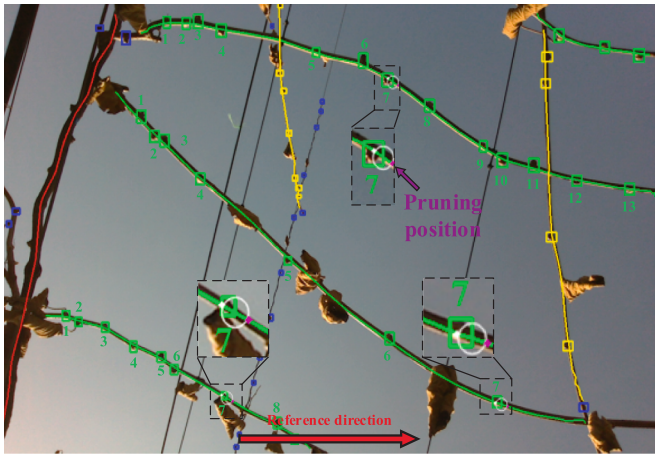


Fig. 7. Pruning position recognition under the CST strategy, where the green, red and yellow line represent skeleton of cane, cordon and lateral cane, respectively. Green, yellow and blue boxes represent dormant buds in cane, lateral cane, and unmatched dormant buds, respectively. The intersection of white offset circle with the skeleton on the left is marked with a white point, and the intersection on the right is marked with a purple point representing pruning position.

(*continued*)

Algorithm 3 (Algorithm of recognizing pruning position under the LCR strategy)

3: **if** ($d > 250$ pixels) **then** // LCR strategy
4: Draw an offset circle with a radius of 30 pixels around *El*;
5: Find an intersection point between the offset circle and *Sl*;
6: *Plcr* ← intersection point
7: **break**
8: **end if**
9: **end for**

2.6.3. Recognition method under the CR strategy

The CR strategy is determined when distance between the endpoint of the first lateral cane on the cane and the endpoint of the cane is less than 250 pixels. The purpose of this strategy is to retain the first lateral cane so that it can produce fruiting shoots in the following season,

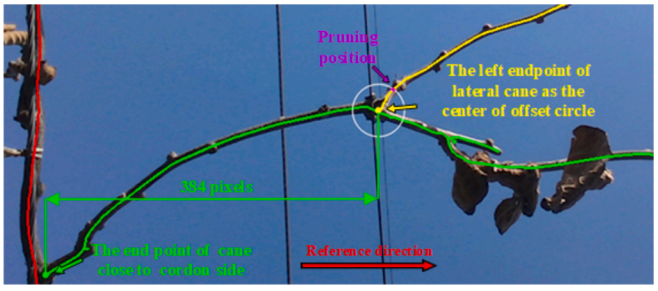


Fig. 8. Pruning position recognition under the LCR strategy, where the green, red and yellow line represent skeleton of cane, cordon and lateral cane, respectively. The white circle is an offset circle with a radius of 30 pixels, drawn from the left endpoint of the lateral cane. The intersection with the lateral cane, marked by a purple dot, represents the LCR pruning position.

thereby ensuring maximum cane vitality. The algorithmic procedure of this strategy is conceptually similar to a combination of the LCR and CST strategies. Specifically, an offset circle is drawn using the endpoint of the first lateral cane as the center, and the pruning position is selected on the cane rather than on the lateral cane. This step is detailed in Algorithm 4

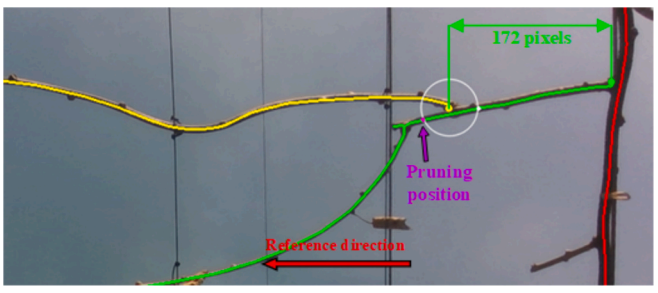


Fig. 9. Pruning position recognition under the CR strategy, where the green, red and yellow line represent skeleton of cane, cordon and lateral cane, respectively. The white circle is an offset circle with a radius of 30 pixels, drawn from the right endpoint of the lateral cane. The intersection with the lateral cane, marked by a purple dot, represents the CR pruning position.

and Fig. 9.

Algorithm 4 (Algorithm of recognizing pruning position under the CR strategy)

Input: Coordinates of current cane skeletons: *Sc*; Coordinates of current cane endpoint: *Ec*; Coordinates lateral cane endpoint: *El*;
Output: Coordinate of pruning position under the CR strategy: *Pcr*;
1: **for** each *El* **do**
2: Compute distance *d* between *El* and *Ec*
3: **if** (*d* < 250 pixels) **then** // CR strategy
4: Draw an offset circle with a radius of 30 pixels around *El*;
5: Find an intersection point between the offset circle and *Sc*;
6: **if** (*Rd* == 'right') **then**
7: *Pcr* ← leftmost point in intersection points
8: **else**
9: *Pcr* ← rightmost point in intersection points
10: **end if**
11: **break**
12: **end if**
13: **end for**

2.7. Performance evaluation

Recognized pruning positions are compared with the judgement of an experienced kiwifruit pruning technician. Original images are presented to technicians, who are asked to mark pruning positions on kiwifruit vines to be pruned based on winter pruning strategy. The accuracy and reliability of method in recognizing pruning positions are evaluated by comparing the output of method with the judgment of the technician. The performance of method is evaluated using pruning position recognition accuracy (*PPRA*) defined in Eq. (1). Where *CT* is the number of pruning positions consistent with the judgment of technician, and *VP* refers to the number of kiwifruit vines to be pruned.

$$PPRA = \frac{CT}{VP} \tag{1}$$

The precision (*P*), recall (*R*), average precision (*AP*) and mean *AP* (m*AP*) are applied to evaluate segmentation and detection performance of YOLO11x-seg and YOLO11x on the test set, respectively (Jiang et al., 2024). All samples are classified into four categories: True Positive *(TP)*, False Positive *(FP)*, True Negative *(TN)* and False Negative *(FN)*. *TP* refers to times that positive samples are recognized to be positive, *FP* refers to times when negative samples are recognized to be positive, *TN* refers to the number of times negative samples are recognized to be negative, and *FN* refers to number of times when positive samples are recognized to be negative. According to the classification of samples, *P* and *R* are defined as shown in Eq. (2) and Eq. (3), respectively. *P* indicates the proportion of relevant detection results among those retrieved, while *R* is the proportion of truly relevant detection results that are correctly recognized. *AP* is an indicator of the overall performance of model, which can be calculated by *P* and *R* in Eq. (4). The m*AP* is the average of *AP* across multiple categories in Eq. (5). Where the value *k* indicates the number of classes of objects.

$$P = \frac{TP}{TP + FP} \tag{2}$$

$$R = \frac{TP}{TP + FN} \tag{3}$$

$$AP = \int_0^1 P_{(R)} dR \tag{4}$$

$$mAP = \frac{1}{k} \sum_{i=1}^{k} AP_i \tag{5}$$

3. Results and discussion

3.1. Segmentation of kiwifruit vines

This study evaluated recent YOLO models, including YOLOv8, YOLO11, YOLO12, and YOLO26. Among them, YOLO26 is the current state-of-the-art model for instance segmentation and object detection. To ensure a reliable and fair performance comparison, each model was independently trained five times under the same experimental settings, and the highest accuracy achieved among the five runs was selected for evaluation. The change trends of segmentation m*AP* for the three models were similar, as shown in Fig. 10. The segmentation m*AP* remained almost unchanged between medium and large parameters of the models. This is mainly because the increase in parameters from the medium to the large is only about 20%, which provides limited improvement in performance. Although YOLO26-seg achieves state-of-the-art performance on benchmark datasets such as COCO (Sapkota et al., 2026), its segmentation m*AP* in this study is generally lower than that of YOLO11-seg. One possible reason is that models optimized for large-scale benchmark datasets may not generalize well to specific agricultural scenarios, such as kiwifruit vine segmentation, due to differences in object structure, visual characteristics, and data distribution. This limitation has also been noted in related studies and is expected to be improved in future model updates. It is expected that this limitation will be improved in future model updates. Therefore, considering accuracy as the primary priority, this study adopts the YOLO11-seg model for vine segmentation.

YOLO11-seg with largest parameter yield high accuracy in vine segmentation. The vine segmentation accuracy increases with model parameters, and the largest model, YOLO11x-seg, achieves an impressive m*AP* of 82.5%, as shown in Table 1. Although it has the slowest segmentation speed, the processing time of 194.4 ms remains acceptable. Although YOLO11x-seg has the slowest segmentation speed of 194.4 ms (0.194 s), its performance is comparable to the 0.184 s required by DeepLabV3 + for wood segmentation reported by Mou et al. (2024) and is substantially faster than the 3.57 s required by Mask R-CNN for pepper branch segmentation reported by Zhang et al. (2024). Furthermore, farmers typically spend approximately 3 s determining how to prune a single vine; therefore, the segmentation speed of YOLO11x-seg is acceptable for practical applications.

The segmentation accuracy of cane and lateral cane may suffer from certain distortions, which can negatively affect the success rate of practical pruning operations. Across all models, the *AP* of lateral cane is lower than that of the cane, and the segmentation accuracy of cane and lateral cane varies significantly. As shown in Fig. 11, misclassification occurs only between cane and lateral cane in all YOLO11-seg models, whereas no such misclassification is observed between cordon and the other vine types. This can be attributed to the fact that cordon has a distinctly different morphology compared to other vine types, which prevents misclassification. In contrast, cane and lateral cane share highly similar morphological characteristics, resulting in persistent misclassification between these two classes. In future work, positional relationships should be considered to better distinguish between cane and lateral cane.

The segmentation of YOLO11x-seg on cordon, cane and lateral cane in Fig. 12 demonstrates compliance with the requirements of winter pruning. YOLO11x-seg is an instance segmentation network. As shown in Fig. 12, it not only segments the branches but also extracts each branch as an individual instance. While some studies applied semantic segmentation networks such as DeepLabV3 + and SegNet to recognize vine or branch (Majeed et al., 2020; Song et al., 2021), these semantic segmentation models make it difficult to individually extract each branch. For pruning tasks, instance segmentation is crucial because it can distinguish vines from the same instance, whereas semantic segmentation treats them as a single region.

Although the segmentation results of YOLO11x-seg show some

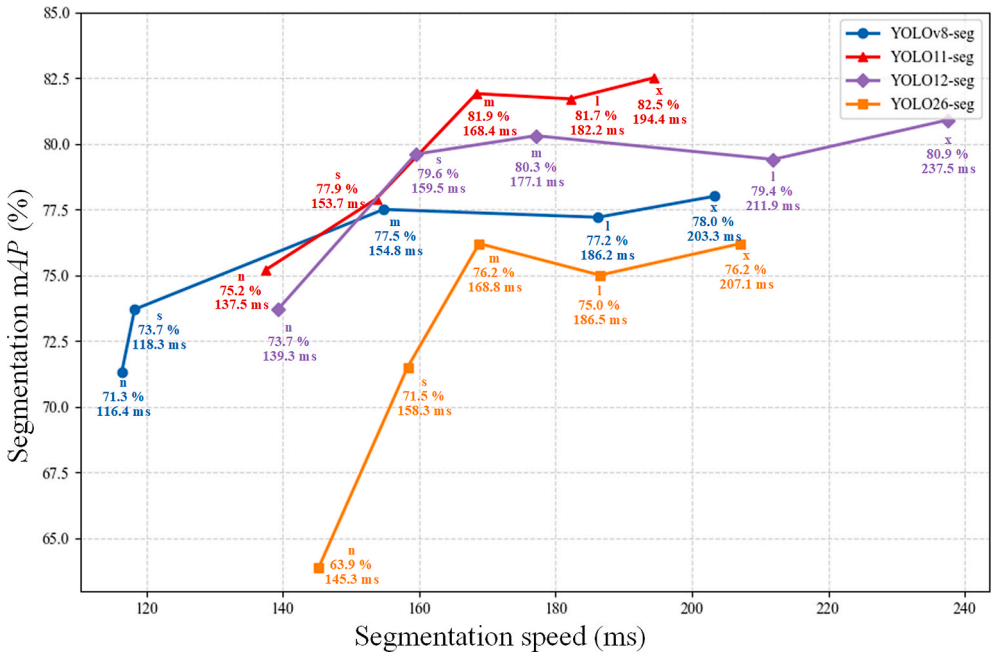


Fig. 10. Segmentation performance of YOLOv8, YOLO11, YOLO12, and YOLO26 models in terms of m*AP* and inference time, where 'n', 's', 'm', 'l' and 'x' represent nano, small, medium, large and extra-large parameters of the models.

Table 1
Segmentation results by YOLO11-seg of different parameters for cordon, cane and lateral cane.

Model	*AP* (%) Cordon	Cane	Lateral cane	m*AP* (%)	Segmentation speed, ms
YOLO11n-seg	84.6	79.5	61.5	75.2	137.5
YOLO11s-seg	85.6	78.2	69.9	77.9	153.7
YOLO11m-seg	83.9	84.9	76.9	81.9	168.4
YOLO11l-seg	82.5	86.8	75.7	81.7	182.2
YOLO11x-seg	83.3	86.1	78.3	82.5	194.4

imperfections, they fully meet the requirements for pruning position recognition. As shown in Fig. 12, in most cases, YOLO11x-seg can segment only vines on the pruning side while leaving opposite side unsegmented, which may indicate that YOLO11x-seg has learned information about vine length. However, this also leads to some very short vines not being segmented even on pruning side, as illustrated by red circle in Fig. 12. In addition, extremely thin vine parts tend to produce disconnected regions, possibly due to information loss during the down sampling process of YOLO11x-seg, which is consistent with the observations of Qi et al. (2023). This issue could be addressed through targeted model improvements in future work.

YOLO11x-seg demonstrates a certain level of generalization ability. In the cross-orchard validation, 17 out of 22 cordons (77.3%), 53 out of 74 canes (71.6%), and 22 out of 162 lateral canes (13.6%) were successfully segmented. As shown in Fig. 13, most thick vines are accurately segmented. However, due to differences in orchard management practices, the orchard used for cross-orchard validation contains a large number of short lateral canes, leading to relatively poor segmentation performance for lateral canes.

3.2. Detection of dormant buds

YOLO11x also performs well in detecting dormant buds. Compared with other YOLO-series models, YOLO11x achieves the highest detection performance, reaching a m*AP* of 89.0% for hidden buds, demonstrating its clear advantage in complex detection scenarios, as shown in Fig. 14. Although YOLO11x does not incorporate specialized structural modifications, its feature extraction capability is comparable to that of dedicated models. Detection accuracies of dormant buds in crops such as apple (Xia et al., 2021), grape (Fernandes et al., 2021), and cherry (Kefalas et al., 2025) generally exceed 90%. However, dormant buds on kiwifruit canes are typically smaller and more inconspicuous, making them significantly more challenging to detect. Under these more demanding conditions, YOLO11x still achieves a m*AP* of 89.0%, which is close to the performance reported for other crops, further highlighting its robustness and effectiveness in detecting small and visually ambiguous targets.

Most dormant buds can be accurately detected in images, indicating that their visual characteristics are sufficiently distinguishable under natural field conditions. Although the color of dormant buds is highly similar to that of vine surface, detection remains feasible because dormant buds usually exhibit subtle geometric features, such as slight protrusions or local shape discontinuities. As shown in Fig. 15, these features provide effective cues for distinguishing buds from surrounding vine tissue. This demonstrates that dormant bud detection does not rely solely on color contrast but instead benefits from detailed structural information present in images.

False detection may occur when objects with appearances similar to dormant buds are present in the scene, which introduces uncertainty into the detection results. Objects such as clips employed to fix canes often have comparable size, shape, and protruding characteristics, making them difficult to distinguish from true dormant buds. Similar challenges have also been reported in pruning related studies on apples and grapes (Lv et al., 2025; Guadagna et al., 2023), indicating that this type of confusion is not specific to a single crop or dataset. This similarity can lead to false positives, particularly in cluttered vineyard environments where auxiliary tools are commonly present. Such errors can directly reduce pruning accuracy and may further lead to incorrect cutting actions. Therefore, filtering methods should be designed in future work to mitigate the influence of these interfering objects.

Dormant buds located on the opposite side of the cordon may also be

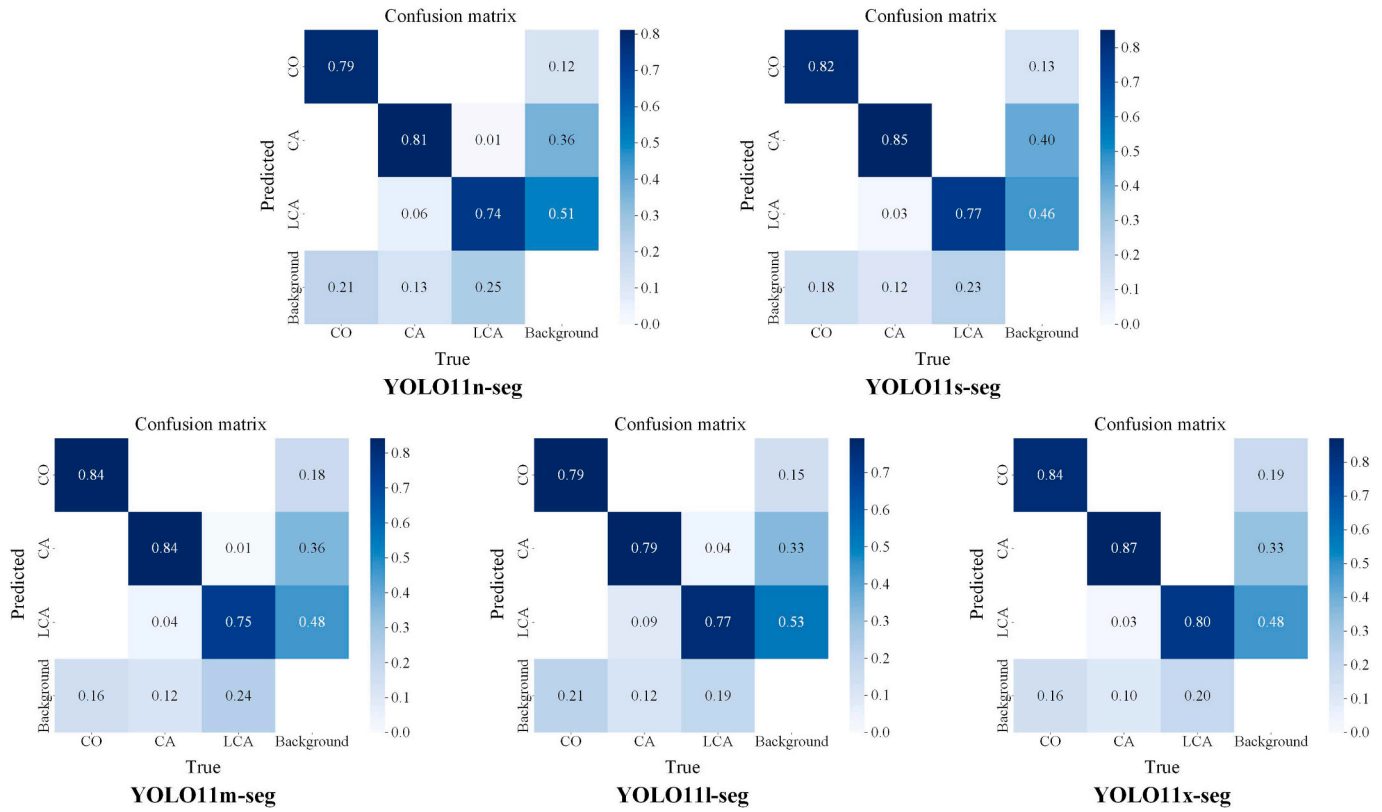


Fig. 11. Confusion matrixes of YOLO11-seg for kiwifruit vine segmentation.

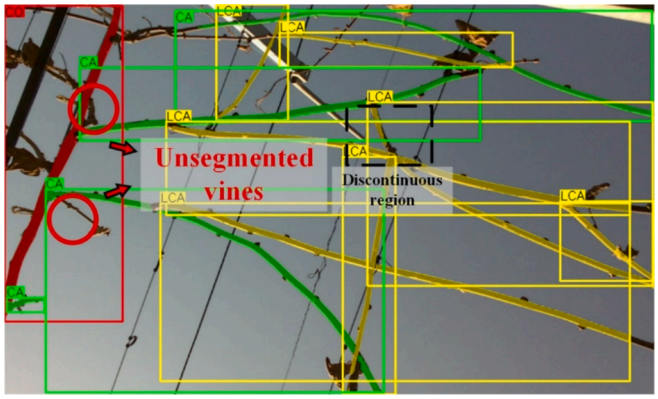


Fig. 12. Kiwifruit canopy image segmented by YOLO11x-seg, where 'CO', 'CA' and 'LCA' represent cordon, cane and lateral cane, respectively, and are visualized as red, green, and yellow polygons.

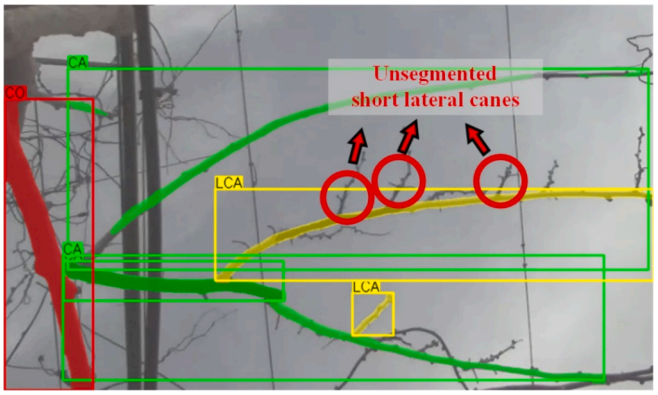


Fig. 13. Kiwifruit canopy image from another orchard segmented by YOLO11x-seg, where 'CO', 'CA' and 'LCA' represent cordon, cane and lateral cane, respectively, and are visualized as red, green, and yellow polygons.

detected due to the absence of explicit positional constraints in the detection process. Buds positioned on the side of the cordon that does not require pruning and were therefore not annotated are still included in the detection results. This behavior indicates that spatial relationships between dormant buds and the cordon, such as relative orientation or side information, are not considered during detection. In practice, convolutional neural networks are known to have limited ability to learn such spatial relationships without additional structural or contextual constraints (Lamichhane et al., 2025). However, since pruning position recognition is determined in a later stage based on ordered bud selection, the inclusion of these buds does not affect the final accuracy of pruning position determination.

YOLO11x further demonstrates robustness. In the cross-orchard validation, 472 out of 636 buds on canes were successfully detected (74.2%). As shown in Fig. 16, buds on short lateral canes are still not detected, mainly due to the lack of representative features of short lateral canes in the training dataset. In well-managed kiwifruit orchards, such short lateral canes are relatively rare. Nevertheless, the model still achieves satisfactory bud detection performance on thicker vines, thereby demonstrating a certain degree of generalization ability.

3.3. *Recognition of pruning position*

The accuracy of pruning position recognition varies across different winter pruning strategies because some dormant buds cannot be detected. In a test of eighteen selected images, pruning positions recognized by method were compared to those determined by pruning technician. As shown in Table 2, the *PPRA*s of the CST, LCR and CR

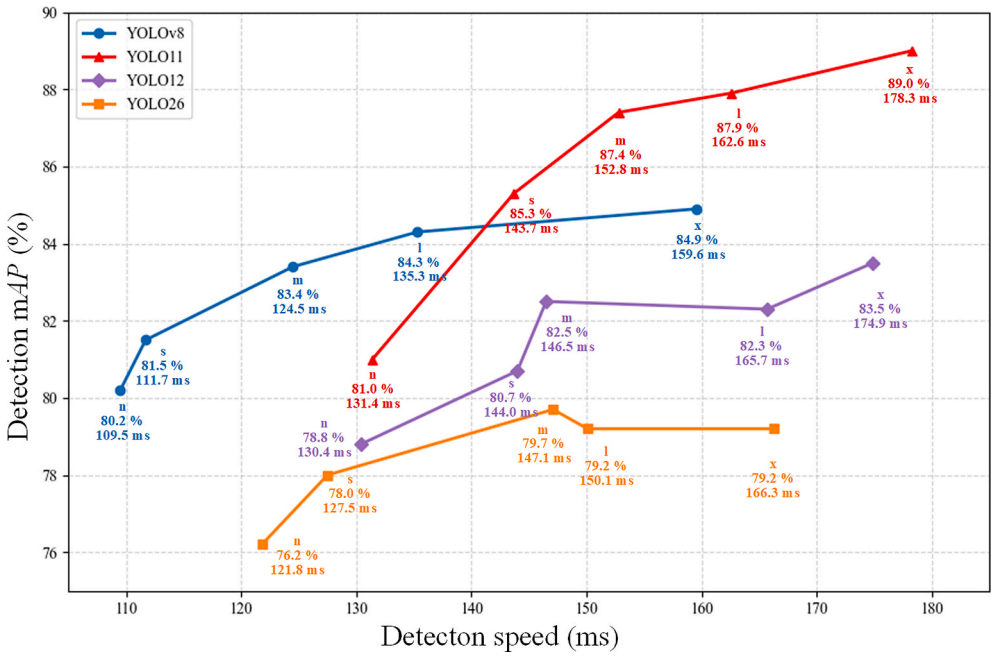


Fig. 14. Detection performance of YOLOv8, YOLO11, YOLO12, and YOLO26 models in terms of m*AP* and inference time, where 'n', 's', 'm', 'l' and 'x' represent nano, small, medium, large and extra-large parameters of the models.

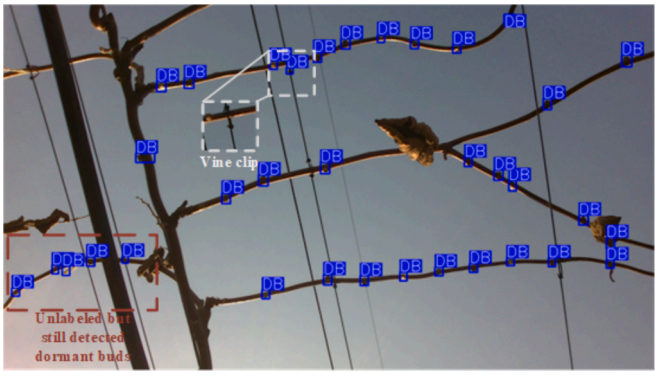


Fig. 15. Kiwifruit canopy image detected by YOLO11x, where 'DB' represents dormant bud.

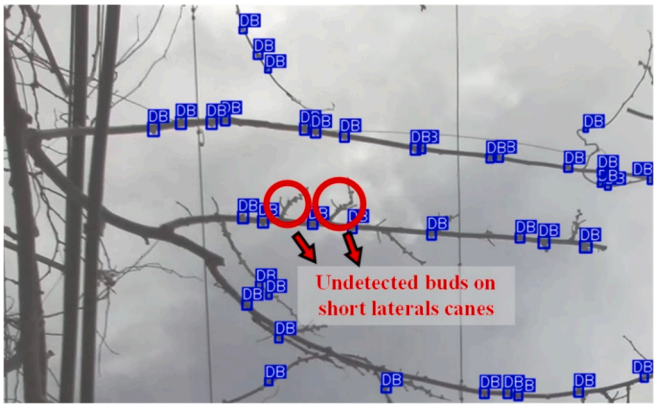


Fig. 16. Kiwifruit canopy image from another orchard detected by YOLO11x, where 'DB' represents dormant bud.

Table 2
Pruning position recognition results of different winter pruning strategies.

Winter pruning strategy	VP	CT	PPRA (%)
CST strategy	22	17	77.3
LCR strategy	11	9	81.8
CR strategy	9	8	88.9
Sum	42	34	80.9

strategies are 77.3%, 81.8%, and 88.9%, respectively. The noticeably lower accuracy of the CST strategy compared with the other two strategies is primarily due to limitations in dormant bud detection. Similarly, the accuracy of dormant bud detection also affects the accuracy of pruning position recognition in grape pruning (Gentilhomme et al., 2023; Williams et al., 2023). Pruning positions under the LCR and CR strategies were recognized by the vine skeleton, which did not depend on dormant bud detection, thus yielding higher accuracy.

In addition, the CR and LCR strategies are distinguished by calculating pixel distance between the endpoints of lateral cane and cane. However, pixel distance does not precisely represent actual physical distance, and variations in the standards of different technicians also introduced some inconsistencies. Future research will focus on improving the accuracy of dormant bud detection and incorporating depth information to estimate the true length between lateral cane and cane. These improvements are expected to reduce discrepancies between pruning position recognition method and human experts and further improve *PPRA* under the CST strategy in future applications.

3.3.1. *Recognition performance under the CST strategy*

Under the CST strategy, misrecognized pruning positions are primarily attributed to the incorrect detection of three types of dormant buds. The first type occurs when YOLO11x fails to detect a bud, as shown in vine-B of Fig. 17. Another type occurs when a clip on the cane is wrongly detected as a dormant bud, as shown in vine-C of Fig. 17. Both types can be addressed by improving dormant bud detection model to enhance its detection accuracy. Final type is more common and difficult

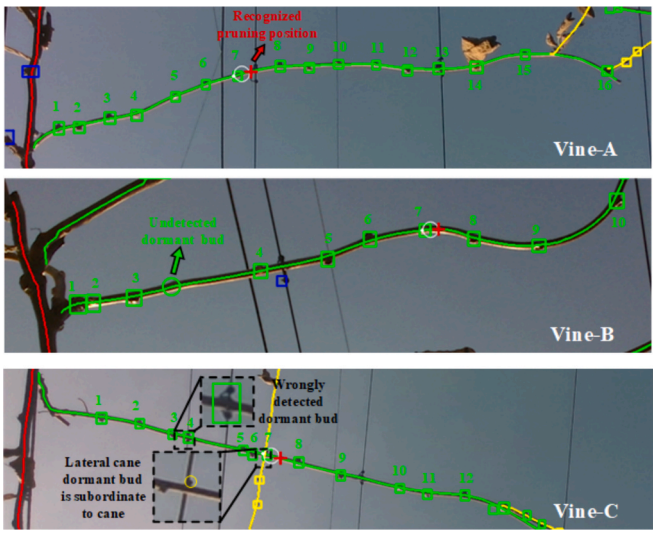


Fig. 17. Recognized pruning position under the CST strategy, where the green, red and yellow lines represent skeleton of cane, cordon and lateral cane, respectively. Green, yellow and bule rectangular boxes represent dormant buds in canes, lateral cane, and unmatched dormant buds, respectively. Red cross represents recognized pruning position.

to address. As illustrated in vine-C of Fig. 17, a dormant bud on a lateral cane is located at the intersection with a cane. This issue may be addressed by capturing multiple images from different positions and comparing whether the relative positions of buds and vines change across the images, or by obtaining more accurate depth information. Fortunately, in this study, selecting the seventh bud in the CST strategy is robust because manual pruning typically retains 6–8 buds, so the impact is limited.

Although pruning position recognition under the CST strategy has relatively low accuracy, it still exhibits a certain degree of robustness. According to the technical regulation for winter pruning of kiwifruit, a single vine should retain six to eight dormant buds under the CST strategy (Wang et al., 2018). The small shift in pruning positions also has a limited effect on kiwifruit yield and quality in the coming year (Cangi and Atalay, 2006). Therefore, even if some dormant buds are wrongly detected or missed, the impact on next year's yield is relatively small.

3.3.2. *Recognition performance under the LCR and CR strategy*

The main source of pruning position recognition errors under the LCR strategy was the incomplete segmentation. As shown in Fig. 18, when a lateral cane was segmented, pruning position was defined by the intersection of a circle and its skeleton mask. Previous studies have not directly addressed the LCR strategy, however, related works on cherry and tomato pruning (You et al., 2023; Feng et al., 2022) recognized pruning positions by offsetting from the intersection of main and lateral vines. In this study, pruning position was instead attained directly from the growth direction of lateral cane, achieving a comparable offset-based effect. In addition, the inaccurate recognition of pruning positions for the LCR strategy was mainly caused by failure to segment lateral canes, as shown in vine-E and vine-F in Fig. 18. These unsegmented lateral canes were generally short and had a similar appearance to unannotated vines.

Unlike the LCR strategy, the CR strategy involves removing cane from previous year while retaining lateral cane close to cordon as cane for next year. Therefore, the method utilized the intersection of drawn circles with the cane skeleton, as shown in Fig. 19. In contrast to the LCR and CST strategies, most pruning positions under the CR strategy are located near image edges, close to cordon. Although camera can be manually adjusted closer to cordon during data collection, robots may not be able to approach it due to the presence of field ridges, resulting in failure to recognize pruning positions under the CR strategy. In the future, when deploying pruning robots, it will be necessary to consider how to expand the robot's field of view to ensure that pruning positions under the CR strategy is visible.

4. Conclusions

This study proposed an automated pruning position recognition method for three different kiwifruit winter pruning strategies, namely cane short-truncation (CST), lateral cane removal (LCR), and cane renewal (CR) pruning. Experimental results indicate that large models achieve high accuracy, with the performance of vine segmentation improving by up to 8%. YOLO11x and YOLO11x-seg achieved the highest m*AP* of 89.0% for dormant bud detection and 82.5% for vine segmentation, respectively. YOLO11x showed a stronger tendency to learn length-related features than planar positional information, which

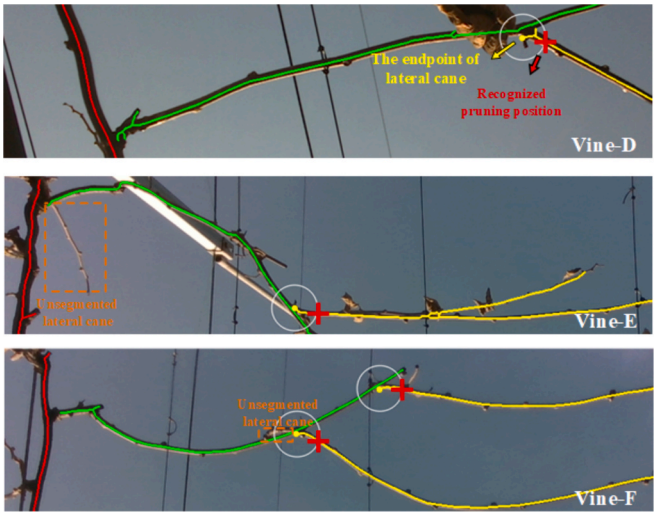


Fig. 18. Recognized pruning position under the LCR strategy, where the green, red and yellow line represent skeleton of cane, cordon and lateral cane, respectively. The white circle is an offset circle with a radius of 30 pixels, drawn from the left endpoint of the lateral cane, drawn as a yellow point. Red crosses represent recognized pruning position.

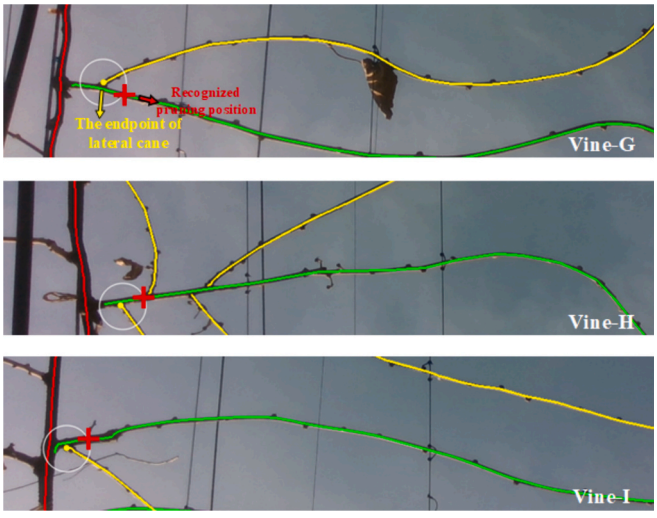


Fig. 19. Recognized pruning position under the CR strategy, where the green, red and yellow lines represent skeleton of cane, cordon and lateral cane, respectively. The white circle is an offset circle with a radius of 30 pixels, drawn from the left endpoint of the lateral cane, drawn as a yellow point. Red cross represents recognized pruning position.

is reflected in its detection of unannotated dormant buds but unable to segment unannotated vines. For discontinuous vine masks, the DBSCAN algorithm helps remove wrongly segmented regions and alleviate the issue of uncertain mask quantities. The pruning position recognition accuracy for CST, LCR and CR strategies were 77.3%, 81.8%, and 88.9%, respectively. Among these pruning strategies, CST strategy remains the most challenging because the recognition model is unable to meet the requirement to accurately detect the accurate number of dormant buds. Although the orchard in this study is managed under standardized cultivation practices, it still contains many occluded regions and extremely thin vines that are difficult for the segmentation model to segment accurately. This consequently leads to most pruning position recognition errors under the LCR and CR strategies. Future work should focus on improving vine segmentation accuracy, as most pruning position errors originate from incorrect segmentation.

Declaration of generative AI in scientific writing

During the preparation of this work the authors used ChatGPT to improve the readability and language of the manuscript. After using this tool, the authors reviewed and edited the content as needed and take full responsibility for the content of the published article.

CRediT authorship contribution statement

Shuolin Kong: Writing – original draft, Methodology, Data curation, Conceptualization. **Bo Jia:** Writing – original draft, Validation, Methodology. **Qichen Huang:** Software, Methodology, Conceptualization. **Juncai Huang:** Software, Methodology. **Rui Li:** Writing – review & editing, Project administration, Data curation. **Bao Zhou:** Supervision, Project administration, Investigation. **Xiancun Zhou:** Validation, Supervision, Software, Resources. **Zhenchao Wu:** Resources, Project administration. **Jinyong Chen:** Validation, Data curation. **Xiaoxu Sun:** Validation, Data curation. **Dateng Zheng:** Funding acquisition, Conceptualization. **Davut Karayel:** Writing – review & editing, Validation. **Dae-Hyun Lee:** Project administration, Formal analysis. **Shen Hin Lim:** Writing – review & editing, Investigation, Conceptualization. **Longsheng Fu:** Writing – review & editing, Supervision, Project administration, Methodology, Funding acquisition, Conceptualization.

Declaration of competing interest

The authors declare that they have no known competing financial interests or personal relationships that could have appeared to influence the work reported in this paper.

Acknowledgements

This work was supported by the National Natural Science Foundation of China (32501786, 32371999) Chinese Universities Scientific Fund (2452026021);National Foreign Expert Project, Ministry of Human Resources and Social Security, China (H20240238, Y20240046); Key Research and Development Program of Shaanxi, China (2024PT-ZCK-27, 2024NC-YBXM-195); Science and Technology Program of Xi'an City, China (24NYGG0035); Central Public-interest Scientific Institution Basal Research Fund, China (1610192023105); National Key Research and Development Program, China (2022YFD1600700); Jiangxi Provincial Key Laboratory of Modern Agricultural Equipment (20242BCC32127).

Data availability

https://github.com/Smart-Ag/Kiwifruit_pruning_image

References

Bai, J., Xing, H., Ma, S., Wang, M., 2019. Studies on parameter extraction and pruning of tall-spindle apple trees based on 2D laser scanner. IFAC-PapersOnLine 52 (30), 349–354. https://doi.org/10.1016/j.ifacol.2019.12.564.

Borrenpohl, D., Karkee, M., 2023. Automated pruning decisions in dormant sweet cherry canopies using instance segmentation. Comput. Electron. Agric. 207, 107716. https://doi.org/10.1016/j.compag.2023.107716.

Cangi, R., Atalay, D.A., 2006. Effects of different bud loading levels on the yield, leaf and fruit characteristics of Hayward kiwifruit. Hortic. Sci. 33 (1), 23–28. https://doi.org/10.17221/3736-HORTSCI.

Carneiro, G.A., Magalhães, R., Neto, A., Sousa, J.J., Cunha, A., 2022. Grapevine Segmentation in RGB Images using Deep Learning. Procedia Comput. Sci. 196, 101–106. https://doi.org/10.1016/j.procs.2021.11.078.

Chen, C., Li, J., Liu, B., Huang, B., Yang, J., Xue, L., 2025. A robust vision system for measuring and positioning green asparagus based on YOLO-Seg and 3D point cloud data. Comput. Electron. Agric. 230, 109937. https://doi.org/10.1016/j.compag.2025.109937.

Chen, Z., Wang, Y., Tong, S., Chen, C., Kang, F., 2024. Grapevine branch recognition and pruning point localization technology based on image processing. Appl. Sci. 14 (8), 3327. https://doi.org/10.3390/app14083327.

Fang, W., Wu, Z., Li, W., Sun, X., Mao, W., Li, R., Majeed, Y., Fu, L., 2023. Fruit detachment force of multiple varieties kiwifruit with different fruit-stem angles for designing universal robotic picking end-effector. Comput. Electron. Agric. 213, 108225. https://doi.org/10.1016/j.compag.2023.108225.

Feng, Q., Wei, C., Li, Y., Wang, B., Chen, L., 2022. Method for identifying tomato plants pruning point using Mask R-CNN. Trans. Chinese Soc. Agric. Eng. 38 (3), 128–135. https://doi.org/10.11975/j.issn.1002-6819.2022.03.015.

Fernandes, M., Scaldaferri, A., Fiameni, G., Teng, T., Gatti, M., Poni, S., Semini, C., Caldwell, D., Chen, F., 2021. Grapevine winter pruning automation: on potential pruning points detection through 2D plant modeling using grapevine segmentation. In: In: IEEE 11th Annual International Conference on CYBER Technology in Automation, Control, and Intelligent Systems, pp. 13–18. https://doi.org/10.1109/CYBER53097.2021.9588303.

Gao, C., He, L., Ding, Y., Murengami, B.G., Chen, J., Zhou, C., Ye, H., Li, R., Fu, L., 2025. A novel multinozzle targeting pollination robot for clustered kiwifruit flowers based on air-liquid dual-flow spraying. J. f. Robot. 42 (5), 2136–2150. https://doi.org/10.1002/rob.22499.

Gentilhomme, T., Villamizar, M., Corre, J., Odobez, J., 2023. Towards smart pruning: ViNet, a deep-learning approach for grapevine structure estimation. Comput. Electron. Agric. 207, 107736. https://doi.org/10.1016/j.compag.2023.107736.

Guadagna, P., Fernandes, M., Chen, F., Santamaria, A., Teng, T., Frioni, T., Caldwell, D. G., Poni, S., Semini, C., Gatti, M., 2023. Using deep learning for pruning region detection and plant organ segmentation in dormant spur-pruned grapevines. Precis. Agric. 22, 1–23. https://doi.org/10.1007/s11119-023-10006-y.

Jiang, H., Gilbert Murengami, B., Jiang, L., Chen, C., Johnson, C., Auat Cheein, F., Fountas, S., Li, R., Fu, L., 2024. Automated segmentation of individual leafy potato stems after canopy consolidation using YOLOv8x with spatial and spectral features for UAV-based dense crop identification. Comput. Electron. Agric. 219, 108795. https://doi.org/10.1016/j.compag.2024.108795.

Karkee, M., Adhikari, B., Amatya, S., Zhang, Q., 2014. Identification of pruning branches in tall spindle apple trees for automated pruning. Comput. Electron. Agric. 103, 127–135. https://doi.org/10.1016/j.compag.2014.02.013.

Kefalas, A., Kalampokas, T., Vrochidou, E., Papakostas, G.A., 2025. A vision-based pruning algorithm for cherry tree structure elements segmentation and exact pruning points determination. Comput. Electron. Agric. 237, 110735. https://doi.org/10.1016/j.compag.2025.110735.

Lamichhane, B.R., Srijuntongsiri, G., Horanont, T., 2025. CNN based 2D object detection techniques: a review. Front. Comput. Sci. 7, 1437664. https://doi.org/10.3389/fcomp.2025.1437664.

Li, X., Liang, B., Liu, S., Li, H., 2021. Pruning decision system for apple tree based on local point cloud and BP neural network. Trans. Chinese Soc. Agric. Eng. 37 (2), 170–176. https://doi.org/10.11975/j.issn.1002-6819.2021.2.020.

Lin, T.-Y., Maire, M., Belongie, S., Hays, J., Perona, P., Ramanan, D., Dollár, P., Zitnick, C.L., 2014. In: Microsoft COCO: Common Objects in Context, in. Springer International Publishing, Cham, pp. 740–755. https://doi.org/10.1007/978-3-319-10602-1_48.

Lv, M., Xu, Y., Miao, Y., Su, W.-H., Lv, M., Xu, Y., Miao, Y., Su, W., 2025. A comprehensive review of deep learning in computer vision for monitoring apple tree growth and fruit production. Sensors 25 (8), 2433. https://doi.org/10.3390/s25082433.

Majeed, Y., Zhang, J., Zhang, X., Fu, L., Karkee, M., Zhang, Q., Whiting, M.D., 2020. Deep learning based segmentation for automated training of apple trees on trellis wires. Comput. Electron. Agric. 170, 105277. https://doi.org/10.1016/j.compag.2020.105277.

Maurya, M., Kumar, S., Kumar, S., Kumari, S., Sahni, R.K., Patel, S.K., Chandra, S., Kumar, N., 2025. Smart vision-based sugarcane bud detection and cutting system for seed generation. Results Eng 27, 106993. https://doi.org/10.1016/j.rineng.2025.106993.

Medeiros, H., Kim, D., Sun, J., Seshadri, H., Akbar, S.A., Elfiky, N.M., Park, J., 2017. Modeling dormant fruit trees for agricultural automation. J. f. Robot. 34 (7), 1203–1224. https://doi.org/10.1002/rob.21679.

Mou, X., Chen, H., Yu, X., Chen, L., Peng, Z., Wang, R., 2024. Lightweight segmentation method for wood panel images based on improved DeepLabV3+. Electronics 13 (23), 4658. https://doi.org/10.3390/electronics13234658.

Özcan, M., Uslu, N., 2010. Effects of pruning practices of shoot development of kiwifruit. Anadolu J. Agric. Sci. 25 (1), 1–9. https://doi.org/10.7161/anajas.2010.25.1.1-9.

Patiyal, V., Rana, V.S., Rana, N., Hashem, A., Abd Allah, E.F., Sharma, S., 2024. Appraisal of extended cane length and fruit thinning strategies on the performance of growth yield and quality of kiwifruit. Heliyon 10 (8), 29546. https://doi.org/10.1016/j.heliyon.2024.e29546.

Patterson, K.J., Currie, M.B., 2011. Optimising kiwifruit vine performance for high productivity and superior fruit taste. Acta Hortic. 913, 257–268. https://doi.org/10.17660/ActaHortic.2011.913.33.

Qi, Y., He, Y., Qi, X., Zhang, Y., Yang, G., 2023. Dynamic snake convolution based on topological geometric constraints for tubular structure segmentation. In: In: 2023 IEEE/CVF International Conference on Computer Vision, pp. 6047–6056. https://doi.org/10.1109/ICCV51070.2023.00558.

Ray, K.K., Kumari, A., Kumar, S., Machavaram, R., Shekh, I., Deshmukh, S.M., Tadge, P., 2025. Guava leaf disease detection using support vector machine (SVM). Smart Agric. Technol. 12, 101190. https://doi.org/10.1016/j.atech.2025.101190.

Ruan, Z., Chang, P., Cui, S., Luo, J., Gao, R., Su, Z., 2023. A precise crop row detection algorithm in complex farmland for unmanned agricultural machines. Biosyst. Eng. 232, 1–12. https://doi.org/10.1016/j.biosystemseng.2023.06.010.

Sapkota, R., Cheppally, R.H., Sharda, A., Karkee, M., 2026. YOLO26: Key Architectural Enhancements and Performance Benchmarking for Real-Time Object Detection. arXiv 2509, 25164. https://doi.org/10.48550/arXiv.2509.25164.

Shen, Q., Zhang, X., Shen, M., Xu, D., 2025. Multi-scale adaptive YOLO for instance segmentation of grape pedicels. Comput. Electron. Agric. 229, 109712. https://doi.org/10.1016/j.compag.2024.109712.

Song, Z., Zhou, Z., Wang, W., Gao, F., Fu, L., Li, R., Cui, Y., 2021. Canopy segmentation and wire reconstruction for kiwifruit robotic harvesting. Comput. Electron. Agric. 181, 105933. https://doi.org/10.1016/j.compag.2020.105933.

Thakur, A., Venu, S., Gurusamy, M., 2023. An extensive review on agricultural robots with a focus on their perception systems. Comput. Electron. Agric. 212, 108146. https://doi.org/10.1016/j.compag.2023.108146.

Wang, Z., Xiao, J., Li, X., Song, F., Han, Z., Xu, J., 2018. Research on kiwi pruning techniques. J. Anhui Agric. Sci. 46(18), 52–53, 56. https://doi.org/10.13989/j.cnki.0517-6611.2018.18.015.

Williams, H., Smith, D., Shahabi, J., Gee, T., Nejati, M., McGuinness, B., Black, K., Tobias, J., Jangali, R., Lim, H., Duke, M., Bachelor, O., McCulloch, J., Green, R., Connor, M., Gounder, S., Ndaka, A., Burch, K., Fourie, J., Hsiao, J., Werner, A., Agnew, R., Oliver, R., MacDonald, B.A., 2023. Modelling wine grapevines for autonomous robotic cane pruning. Biosyst. Eng. 235, 31–49. https://doi.org/10.1016/j.biosystemseng.2023.09.006.

Xia, X., Chai, X., Zhang, N., Sun, T., 2021. Visual classification of apple bud-types via attention-guided data enrichment network. Comput. Electron. Agric. 191, 106504. https://doi.org/10.1016/j.compag.2021.106504.

You, A., Parayil, N., Krishna, J.G., Bhattarai, U., Sapkota, R., Ahmed, D., Whiting, M., Karkee, M., Grimm, C.M., Davidson, J.R., 2023. Semiautonomous precision pruning of upright fruiting offshoot orchard systems: an integrated approach. IEEE Rob. Autom. Mag. 30 (4), 10–19. https://doi.org/10.1109/MRA.2023.3309098.

Zhang, C., Zhang, Y., Liang, S., Liu, P., 2024. Research on key algorithm for Sichuan pepper pruning based on improved Mask R-CNN. Sustainability 16 (8), 3416. https://doi.org/10.3390/su16083416.